Adsorption (2013) 19:121–129
DOI 10.1007/s10450-012-9427-x

Multilayer adsorption equilibrium model for gas adsorption on solids

Sébastien Thomas · Pierre Schaetzel

Received: 22 October 2011 / Accepted: 17 September 2012 / Published online: 11 October 2012

Abstract Adaptation of the ENSIC model to physisorption of nitrogen or argon on a solid surface first led to a 3 parameters model called multilayer adsorption equilibrium model (MAE model). One of these parameters is related to the formation of a multilayer of adsorbate on the solid surface. Exploitation of data from the literature pointed out that this parameter does not depend on the nature of the solid surface and an average value was calculated in the case of N_2 and Ar. As a consequence, the MAE model can be considered as a 2 parameters model. Linearization of the model was established allowing an easy determination of surface areas of macroporous and some mesoporous solids. Fitting of isotherms of meso and macroporous solids has led to promising results compared to the ones obtained with the BET model. Moreover, adaptation of this model to microporous solids can also be used for an uncomplicated determination of porous volume and external surface. Results obtained from data of the literature were close to those obtained with the *t*-plot model.

Keywords Adsorption isotherm · Surface area · Pore volume · Mesoporous solid · Microporous solid

1 Introduction

Porous materials are of great interest in many fields such as heterogeneous catalysis (Ramsay 1998), separation processes such as chromatography (Thielmann et al. 2001; Rodrigues 1997) or membranes (Blanco et al. 2006; Yan et al. 2004), drug hosts (Ramila et al. 2003; Anglin et al. 2008) or sensors (Leite et al. 2010; Whalley et al. 2001). In fact, in addition to attractive chemical surface properties, high surface areas and specific pore systems are often required to enhance solid properties. Characterization and quantification of these two last parameters are generally obtained from physisorption isotherms (Sing et al. 1985), which have been the subject of many reviews (Ramsay 1998; Leofanti et al. 1998; Sing and Williams 2005; Rodrigues et al. 1989).

Among models describing the adsorption isotherm, the BET model, developed by Brunauer, Emmett and Teller (Brunauer and Emmett 1938; Brunauer 1945), is the most widely used. It allows an easy determination of the surface area of non-microporous solids. This model is based on uniformity of the surface and on the absence of lateral interactions of adsorbed molecules. Moreover, this model implies that the second and further layers can start to build up before the completion of the first one. Based on these hypotheses, adsorption and desorption rates can be expressed as function of the partial pressure and of the proportion of each adsorbed layer. At equilibrium, adsorption and desorption rates on each layer are supposed to be equal. This results in a 2 parameters equation:

$$V_{ads} = \frac{\frac{P}{P_0} \cdot C \cdot V_m}{(1 - \frac{P}{P_0}) \cdot (1 + (C - 1) \cdot \frac{P}{P_0})} \quad (1)$$

where V_{ads} stands for the adsorbed volume per gram of sample (generally expressed in $cm^3\,STP\,g^{-1}$), V_m for the volume of gas needed to cover all the surface of one gram of sample with a monolayer, P the pressure of the gas phase and P_0 the vapor pressure of the adsorbate in the working conditions (generally equals to 1 atm in the usual case of nitrogen at 77 K). C is related to the difference between the heat of adsorption on free surface and heat of condensation

S. Thomas (✉) · P. Schaetzel
Laboratoire Catalyse et Spectrochimie, ENSICAEN, Université de Caen, CNRS, 6 Bd Maréchal Juin, 14050 Caen, France
e-mail: sebastien.thomas@ensicaen.fr
Fax: +33-23-1452822

and so to the interaction strength between the adsorbent-adsorbate.

Equation (1) can be linearized as:

$$\frac{\frac{P}{P_0}}{V \cdot (1 - \frac{P}{P_0})} = \frac{1}{CV_m} + \frac{C-1}{CV_m} \cdot \frac{P}{P_0} \tag{2}$$

which allows determining V_m and C. The surface area of the sample can be deduced from V_m assuming a complete coverage of the sample with each molecule occupying the same surface. A value of 16.2 Å^2 is generally assumed for the cross-sectional area of a nitrogen molecule (σ_{N2}) (Mikhail and Brunauer 1975) but this value may depend on the type of surface (Jelinek and Kovhts 1994; Amati and Kovats 1987). The BET model can be applied to a mesoporous or macroporous solid in a range of relative pressure of 0.05–0.3 (Gregg and Sing 1982). In fact, heterogeneities of the surface and/or presence of micropores, even in small amounts, can lead to a non linear BET plot for very low relative pressures. At higher pressure, capillary condensation may occur depending on the pore size distribution of the sample.

Another model widely used is the t-plot which is more adapted to microporous solid. This model was proposed by Lippens and DeBoer in 1965. It is based on the fact that when non capillary condensation occurs, the volume adsorbed can be expressed by the surface area of the solid multiplied by the average thickness of the adsorbed layer. This average thickness has been seen to be quasi independent of nature of the solid surface but depends only on the pressure (Gregg and Sing 1982). Several models or semi empirical equations have been developed to express the evolution of this average thickness (t) as a function of the reduced pressure (P/P_0) for different classes of solids. Among them, equations proposed by Halsey in 1948 and Harkins and Jura in 1944 are the most widely used:

$$\text{Harkins-Jura:} \quad t = \left[\frac{13.99}{0.34 - \log(\frac{p}{p_0})}\right]^{1/2} \tag{3}$$

$$\text{Halsey:} \quad t = 3.54 \cdot \left[\frac{-5}{\log(\frac{p}{p_0})}\right]^{1/3} \tag{4}$$

where t is expressed in Å.

The plot of the adsorbed volume as a function of the average thickness should lead to a straight line passing through the origin with a slope proportional to the surface area of the sample.

In the case of microporous solids (Everett 1998), filling of the pores occurs at relatively low pressure, which has for consequence a non linearity between adsorbed volume and calculated average thickness. When the micropores are completely filled, adsorption is believed to occur only on external surface and the slope of the line obtained is then related to this external surface. Moreover, extrapolation to $t = 0$ allows estimating the microporous volume. The same kind of data treatment can also be applied to mesoporous solids in a well-chosen range of 't'.

The t-plot method is widely favored to calculate microporous volume and external surface but its use can face two major difficulties: the choice of the equations to estimate t (Lecloux and Pirard 1979) can lead to non negligible differences in the determination of porous volume and external surface; for solids with a broad distribution of pore size, it can be difficult to find a linear part on the t-plot curve (Storck et al. 1998).

2 Description of the MAE model

2.1 ENSIC model

Sorption of solvents in polymers is a well studied phenomenon (Astarita and Joshi 1978; Robinson et al. 2004) as it plays a major role in transport processes through dense membranes. Flory-Huggins thermodynamics theory is the most used approach to model this phenomenon (Flory 1953). However even this model requires only one parameter, theoretically constant (the so-called polymer solvent interaction parameter); numerous studies have shown that this parameter depends on polymer concentration (Favre et al. 1993; Moore and Shuttleworth 1963). This leads to complex expressions with numerous adjustable parameters which make this model doubtful in some cases.

In the 90's Favre et al. have proposed a model called 'ENgaged Species Induced Clustering' (ENSIC) aiming to link solvent volume fraction in the polymer matrix to the solvent activity (Favre et al. 1993, 1996).

The ENSIC model considers the probability of insertion of one non-polymeric molecule (e.g. gas, vapor or solvent) in a polymer/solvent matrix containing only two types of species, one being present only in the condensed phase. The key parameters are the elementary affinity between the non-polymeric species and either a polymer segment (k_p) or a previously sorbed solvent molecule (k_s). As a consequence, the basic mechanism underlying the ENSIC model development is related to two distinct modes of sorption: a sorbed solvent molecule can either be in interaction with the polymer or in interaction with a previously sorbed solvent molecule. Sorption of a solvent molecule can be seen as an increase of the solvent volume fraction in the polymer matrix. This model was successfully applied to many systems (Favre et al. 1996) involving various polymers (e.g. polydimethylsiloxane and polyethylene) and various solvents (e.g. water and toluene).

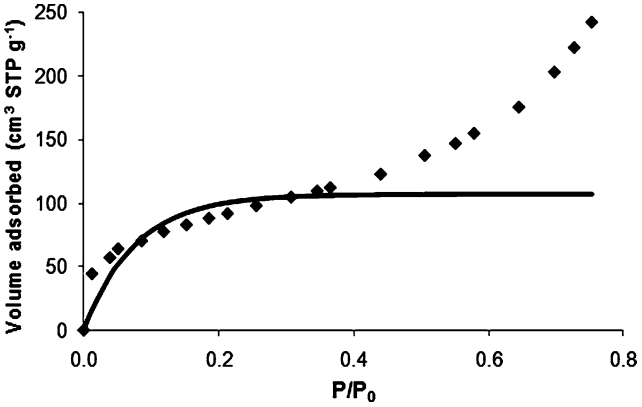

Fig. 1 Fit of the ENSIC model to the experimental isotherm, obtained with macroporous silica sample TK800 (Payne et al. 1973) from $P/P_0 = 0$ to 0.5

2.2 MAE model

Extrapolation of this model to physisorption and to surface adsorption is not straightforward because this phenomenon occurs on the surface whereas sorption of solvent in a polymer can be seen in a volumetric way. In fact, Fig. 1 shows that ENSIC model does not describe correctly the experimental results of a physisorption isotherm on a macroporous silica (Payne et al. 1973).

However, application of the ENSIC model on the system sorbent + adsorbate has been attempted taking into account these differences. The starting equation of ENSIC model was adapted for the 'Multilayer Adsorption Equilibrium Model' (MAE model) developed here. Adsorption on free surface sites or on a previously adsorbed molecule is considered. It leads to (5):

$$dn_{ads} = (k_p \cdot n_p + k_s \cdot n_s) \cdot d\frac{P}{P_0} \tag{5}$$

where:

- n_{ads} stands for the adsorbed amount in mole per gram of solid
- n_p stands for the number of adsorption sites remaining free on the surface of the solid per gram of solid at a pressure P
- n_s stands for the number of adsorption sites occupied by the adsorbate on the surface of the solid per gram of solid at a pressure P
- k_p corresponds to the adsorption coefficient of adsorbate on the free solid surface (unitless)
- k_s corresponds to the adsorption coefficient of adsorbate on previously adsorbed molecule (unitless)

It is important to notice that it is expected that $k_s < k_p$, i.e. the adsorption is more favored on the free solid surface than on a previously adsorbed molecule (Brunauer and Emmett 1938). It should also be noted that, in the absence of capillary condensation, and for a given sorptive gas, the sum $n_p + n_s$ (total number of sites on the surface of the solid per gram of sample), expressed as n_m, only depends on the solid and not on the pressure.

One major difference of MAE model compared to ENSIC model is that the decrease of the amount of free adsorption sites on the surface has to be taken into account. This phenomenon can be expressed as:

$$dn_p = -k_p \cdot n_p \cdot d\frac{P}{P_0} \tag{6}$$

Since we consider a clean surface at $P = 0$, integration of (6) leads to (7):

$$n_p = n_m \cdot e^{-k_p \cdot \frac{P}{P_0}} \tag{7}$$

As a consequence (5) can be expressed now as (8):

$$dn_{ads} = n_m\left[k_p \cdot e^{-k_p \cdot \frac{P}{P_0}} + k_s\left(1 - e^{-k_p \cdot \frac{P}{P_0}}\right)\right] \cdot d\frac{P}{P_0} \tag{8}$$

Integration from pressure 0 to P leads to a 3 parameters relation between the amount of adsorbate and the relative pressure (9):

$$n_{ads} = n_m\left[\left(1 - \frac{k_s}{k_p}\right)\left(1 - e^{-k_p \frac{P}{P^\circ}}\right) + k_s \frac{P}{P^\circ}\right] \tag{9}$$

This expression can be simplified for very low pressure into a linear law (10) which is in agreement with a Henry law (Hill 1952)

$$n_{ads} = n_m k_p \frac{P}{P^\circ} \tag{10}$$

For intermediate and high relative pressure, the solid is almost covered by the adsorbate and adsorption occurs only on an adsorbate layer with a linear trend (11):

$$n_{ads} = n_m\left(1 - \frac{k_s}{k_p} + k_s \frac{P}{P^\circ}\right) \tag{11}$$

3 Application of MAE model to macro- and mesoporous solids

3.1 Physisorption with nitrogen

For macroporous solids, Eq. (11) can be used in the linear part of the isotherm, generally for values of P/P_0 between 0.3 and 0.6. In fact, at lower pressure, the surface is generally not entirely covered by the adsorbate. At higher pressure, capillary condensation (not predicted by the model) can occur, which excessively increases the adsorbate amount. For mesoporous samples, a P/P_0 range has to be found between the total coverage of the surface and the beginning of the hysteresis corresponding to the capillary condensation in the smaller mesopores. This range is generally found before the inflexion point (Fig. 2).

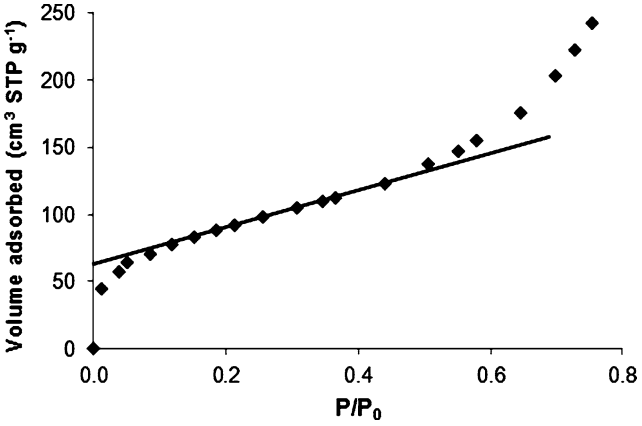

Fig. 2 Linear part of TK800 sample isotherm (data from Payne et al. 1973)

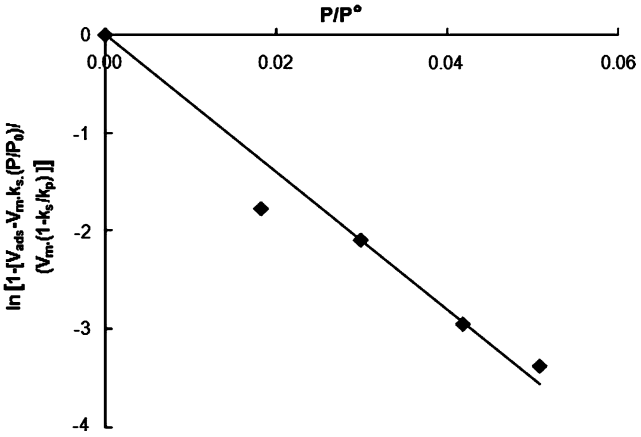

Fig. 3 MAE model line at low pressure for TK800 sample (Payne et al. 1973)

The parameters of the straight line obtained with (11) (Fig. 3) allow determining $n_m \cdot k_s$ (slope) and $n_m(1 - \frac{k_s}{k_p})$ (y-intercept value). In a first approximation, one can neglect the term $\frac{k_s}{k_p}$ thus considering the y-intercept value as n_m. The adsorption coefficient k_s can then be expressed as the slope/y-intercept ratio.

A more precise way to determine the parameters is to subtract the linear part expressed by Eq. (10) from the isotherm values at low pressure. Dividing the resulting values by $n_m \cdot (1 - \frac{k_s}{k_p})$, previously determined as the y-intercept of the intermediate pressure line, leads to Eq. (12):

$$\frac{n_{ads} - n_m \cdot k_s \cdot \frac{P}{P_0}}{n_m \cdot (1 - \frac{k_s}{k_p})} = \left(1 - e^{-k_p \cdot \frac{P}{P_0}}\right) \tag{12}$$

where k_p can then be deduced by plotting

$$\ln\left[1 - \frac{n_{ads} - n_m \cdot k_s \cdot \frac{P}{P_0}}{n_m \cdot (1 - \frac{k_s}{k_p})}\right]$$

as a function of P/P_0 for low reduced pressure values (Fig. 3). Values of k_s and n_m can then be more accurately inferred with Eq. (11) and without neglecting $\frac{k_s}{k_p}$.

To identify more clearly the range which could be used for this so called 'linear part', it can be helpful to plot the first derivate of the isotherm (Fig. 4). This allows an estimation of the range of the linear part (from $P/P_0 = 0.15$ to 0.40 in the case of Fig. 4).

Parameters k_s and k_p can then be calculated for different ranges of relative pressure. Values obtained, reported in Table 1, do not vary significantly with the range chosen.

Determination of the values of k_p, k_s and n_m allows rebuilding the whole isotherm. The linear trend of the isotherm is modeled in a larger range of pressure by the MAE model than by the BET model (Fig. 5 for TK800 sample of Payne et al. 1973). For low relative pressures, both models lead to similar values.

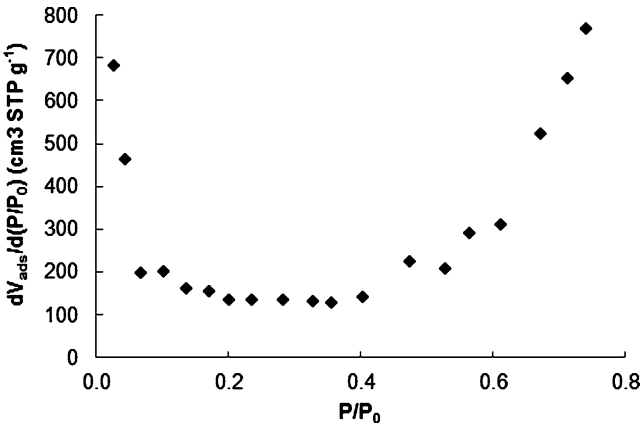

Fig. 4 First derivative of the isotherm of a mesoporous silica from Payne et al. (1973)

Table 1 k_s and k_p parameters and correlation coefficients of MAE line at middle pressure calculated from different ranges of relative pressure for a mesoporous silica from Payne et al. (1973)

Range	k_s	k_p	r^2
0.10–0.35	2.14	52	0.99867
0.10–0.40	2.16	51	0.99887
0.10–0.45	2.15	51	0.99931
0.15–0.40	2.09	49	0.99958
0.20–0.40	2.03	48	0.99997
0.20–0.35	2.03	48	0.99999
0.20–0.45	2.07	49	0.99982
0.25–0.45	2.09	49	0.99968

Distinction between adsorption on solid surface and multilayer formation can be appreciated by plotting the modeled isotherm with $k_s = 0$ (no multilayer formation) and with $k_p = 0$ (adsorption on the solid surface no taken into account) (Fig. 6).

The surface area can be derived from the MAE model (S_{MAE}) in a similar way to that used in the BET one (13):

$$S_{MAE} = n_m \cdot \sigma_{ads} \cdot N_A \tag{13}$$

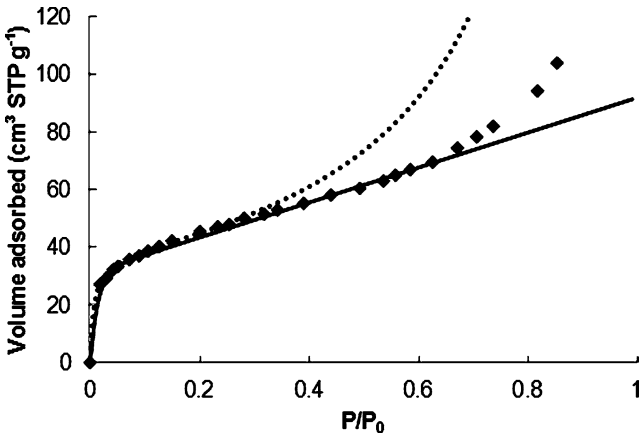

Fig. 5 Comparison of the experimental physisorption isotherm on TK800 sample from Payne et al. (1973) (*diamonds*) with isotherms calculated with BET model (*dotted line*) and MAE model (*full line*)

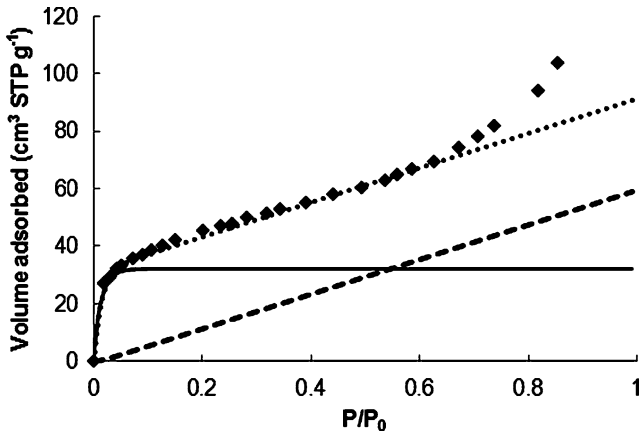

Fig. 6 Comparison of the experimental physisorption data on TK800 sample from Payne et al. (1973) (*diamonds*) with isotherms calculated from MAE model (*dotted line*) with $k_s = 0$ (*full line*) and $k_p = 0$ (*dashed line*)

with σ_{ads} the surface occupied by one adsorbate molecule on the surface of the solid.

Adsorption isotherms data with nitrogen at 77 K, for samples differing in surface and composition, were found in the literature. These results were used to evaluate parameters in the MAE model (Table 2).

It should be noted that values obtained for k_s are similar for all the samples i.e. they are not strongly depending on the surface or its chemical nature (Fig. 7). In the MAE model, the coefficient k_s is related to the adsorption of the gas on an adsorbed layer. For one temperature, if the model is coherent, this coefficient should be independent of the solid and only dependent of the nature of the adsorbed gas. We have fitted 17 experimental N_2 adsorption data at 77 K. The mean k_s coefficients are found equal to 2.00 with a standard deviation of 0.03. This is clearly coherent with definition of the k_s coefficient in the MAE model. With this observation, the model which was built as a three parameters model can be

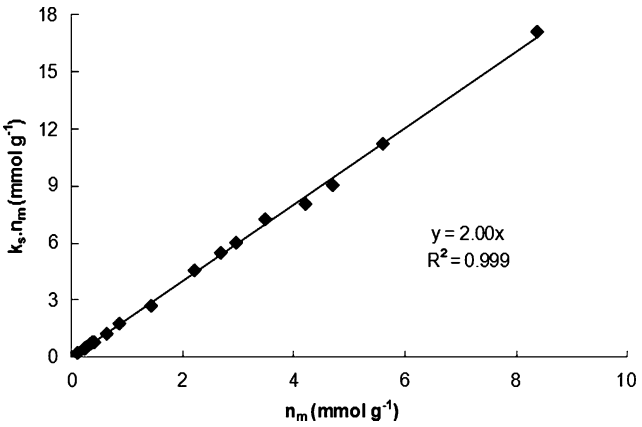

Fig. 7 Determination of average k_s value for samples presented in Table 1

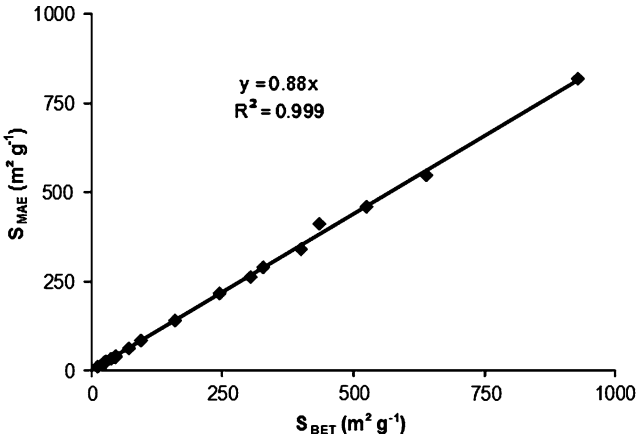

Fig. 8 Comparison between surface area values determined by the MAE and BET models, for the samples presented in Table 1

considered as a two parameters model like the BET equation with $k_s = 2.00$ for N_2. Alternatively, if one uses the three parameters to analyze his experimental results, the k_s obtained could be a good test of the verification of MAE model.

In these conditions, n_m as well as S_{MAE} can be deduced directly with Eq. (11) from the slope of the straight line for intermediate P/P_0 values. When comparing surface values calculated from MAE and BET models, a linear correlation can be observed (Fig. 8), indicating a good correspondence of the two models with an overestimation of the BET model or an underestimation of MAE. Anyway, MAE model allows determining the specific surface area using only a few points in the intermediate reduced pressure range and prior to the development of the capillary condensation phenomenon.

The data presented in Table 2 shows that the ratio $\frac{k_s}{k_p}$ is generally lower than 0.05 and can be neglected in Eq. (11) as a first approximation. This ratio is related to the comparison of the adsorption modes (on a free surface *vs*. on a covered site). As a consequence, a correlation has been attempted be-

Table 2 S_{MAE}, k_p and k_s values calculated ; S_{BET} and C obtained from nitrogen adsorption isotherm at 77 K on various samples from the literature

Reference	Sample	S_{BET} ($m^2\,g^{-1}$)	C	S_{MAE} ($m^2\,g^{-1}$)	k_p	k_s
Payne et al. (1973)	Silica TK 800	160	128	140	70	1.88
	Mesoporous silica gel B	328	74	289	48	2.03
Keller et al. (1999)	SiC	25	133	23	63	1.98
de Boer et al. (1966)	Alumina	245	111	216	50	2.06
Emmett and Brunauer (1937)	Iron Synthetic Ammonia Catalyst	25	92	23	42	1.94
Pomonis et al. (2005)	SiO_2	928	58	818	33	2.04
Bartoszek et al. (2009)	Mesoporous silica-alumina	435	166	411	70	1.91
Serwicka (2000)	V_2O_5–WO_3/TiO_2-fresh	47	152	40	68	1.90
	V_2O_5–WO_3/TiO_2-aged	46	136	37	77	2.08
Witoon et al. (2011)	Meso-macroporous silica MSI-3	400	172	340	82	2.08
	Meso-macroporous silica HS-3	304	108	262	51	2.04
Trammell et al. (2011)	Bis(trimethoxysilylethyl)benzene	525	79	459	52	1.92
Izquierdo-Barba et al. (2011)	SBA-15	639	162	547	79	2.00
Marinovic et al. (2011)	Bentonite S_0	28	47	25	29	1.95
	Bentonite SA	38	66	33	37	2.06
Anu Prathap and Srivastava (2011)	CeO_2 calcined at 923 K	72	50	62	30	1.93
	CeO_2 calcined at 823 K	95	63	84	41	2.05

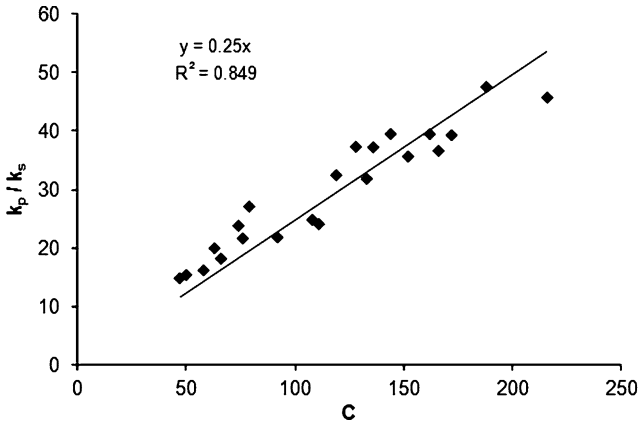

Fig. 9 k_p/k_s ratio as a function of the 'C' BET parameter, for samples presented in Table 2

tween the ratio $\frac{k_s}{k_p}$ and the 'C' parameter of the BET model (Fig. 9).

Even though one can argue on the accuracy of the determination of 'C' and k_p, a linear trend can be observed in Fig. 9, pointing to the similarity between the two models.

3.2 Physisorption with argon

Argon adsorption isotherms were also processed (Table 3). The value of the cross-sectional area of an argon molecule (σ_{Ar}) used for the calculation was 13.8 Å^2 (McClellan and Hainsberger 1967). A linear trend between C and the $\frac{k_s}{k_p}$ ratio was also observed (not shown).

Similarly as for nitrogen, surfaces estimated by MAE model were around 20 % lower than those determined by BET method. The values obtained for k_s were similar for all the samples (*ca.* 2.4) but different from the one calculated in the case of nitrogen (*ca.* 2.0) indicating the specificity of each molecule rather than the influence of the solid in the formation of multilayers.

4 Application to microporous solids

For microporous solids, pore-filling occurs at very low P/P_0 and the Eq. (9) can be adapted to Eq. (9′) for higher reduced pressure:

$$n_{ads} = n_{micro} + n'_m\left[\left(1-\frac{k_s}{k_p}\right)\left(1-e^{-k_p\frac{P}{P_0}}\right)+k_s\frac{P}{P_0}\right] \quad (9')$$

where n_{micro} corresponds to the amount of adsorbate needed to fill up the micropores and n'_m to the number of surface sites non present in the microporosity (i.e. on the external surface).

At intermediate pressures, Eq. (9′) can be simplified as expressed in Eq. (14) and leads to the determination of the microporous volume:

$$n_{ads} = n_{micro} + n'_m\left[\left(1-\frac{k_s}{k_p}\right)+k_s\frac{P}{P_0}\right] \quad (14)$$

As previously mentioned, the $\frac{k_s}{k_p}$ ratio is generally found to be less than 0.05 (Table 2) and it can then be neglected in Eq. (14). Moreover, estimating k_p is in that case difficult,

Table 3 S_{MAE}, k_p and k_s values calculated; S_{BET} and C obtained from argon adsorption isotherm at 77 K on various samples from the literature

Reference	Sample	S_{BET} ($m^2\,g^{-1}$)	C	S_{MAE} ($m^2\,g^{-1}$)	k_p	k_s
Ruzicka and Kudlacek (1964)	Regenerated cellulose	64	28	54	24	2.48
Selles-Perez and Martin-Martinez (1992)	Carbon Ap	7.3	61	6.1	56	2.37
Payne et al. (1973)	Silica TK 800	121	36	98	28	2.35
	Nonporous hydroxylated silica	137	36	112	30	2.34
	Mesoporous silica gel B	253	33	202	30	2.52

Table 4 Microporous volume ($V_{micro\ MAE}$) and external surface ($S_{ext\ MAE}$) values of various samples from the literature calculated by MAE model. Comparison with the values calculated in the reference ($V_{micro\ ref}$ and $S_{ext\ ref}$)

Reference	Sample	$V_{micro\ MAE}$ (cm^3 STP g^{-1})	$S_{ext\ MAE}$ ($m^2\,g^{-1}$)	$V_{micro\ ref}$ (cm^3 STP g^{-1})	$S_{ext\ ref}$ ($m^2\,g^{-1}$)
Passe-Coutrin et al. (2008)	Activated carbon VetH_20	0.34	290	0.36	291
	Activated carbon P0.5	0.42	186	0.45	153
	Activated carbon P1	0.36	536	0.39	535
	Activated carbon P1.5	0.20	521	0.22	536
Scherdel et al. (2010)	Carbon pyrolyzed at 1000° C	0.24	100	0.25	90
	Carbon pyrolyzed at 1500° C	0.07	118	0.09	96
Sergio et al. (2006)	Montmorillonitic Clay M > 450	0.11	39	0.11	27
	Montmorillonitic Clay M < 250	0.15	77	0.17	37
Frackowiak (2006)	KOH activated carbon	0.73	453	0.80	374
Dimitrov et al. (2011)	ZSM-12 zeolite-parent	0.11	54	0.11	62
	ZSM-12 zeolite-desilicated	0.09	159	0.11	141
Guzmán-Castillo et al. (2011)	Y zeolite-F-1C	0.25	48	0.26	55
	Y zeolite-MMZ-34C	0.28	94	0.28	115
	Y zeolite-MMZ-38C	0.20	205	0.20	253
Méndez et al. (2006)	Petroleum Coke-Norit	0.48	65	0.51	21

because filling of the micropores and progressive coverage of the surface occur simultaneously. Using the parameters of the linear section of the adsorption isotherm at intermediate pressures, n_{micro} can then be expressed as follows:

$$n_{micro} = y\ intercept - \frac{slope}{k_s} \tag{15}$$

with $k_s \approx 2.0$ for N_2 at 77 K as previously determined.

The microporous volume can then be easily calculated assuming that the molar volume of the adsorbate in the micropores is equal to the one of the liquid. The amount of non-microporous adsorption sites (non-microporous surface, so called external surface) can also be obtained from Eq. (16):

$$n'_m = \frac{slope}{k_s} \tag{16}$$

Nitrogen isotherm data on microporous solids extracted from the literature have been examined using the MAE model. The results are summarized in Table 4.

A good agreement is obtained for microporous volume by the MAE model and by the t-plot method (Fig. 10). It is important to stress that microporous volumes derived from MAE model are obtained with only few points in the intermediate reduced pressure range and with simpler calculation than in the t-plot method. The underestimation of microporous volume by the MAE model when compared to the t-plot may be partially associated to the fact that the $\frac{k_s}{k_p}$ ratio has to be neglected in Eq. (14).

Figure 11 depicts the comparison between the external surfaces determined by the MAE model and by the t-plot model. The results show a good agreement between the external surface values deduced from the MAE model and those found in the corresponding articles.

5 Conclusions

Adaptation of the ENSIC model to physisorption of nitrogen or of argon on solid surfaces leads to a 2 parameters model (MAE model) allowing an easy determination of surface

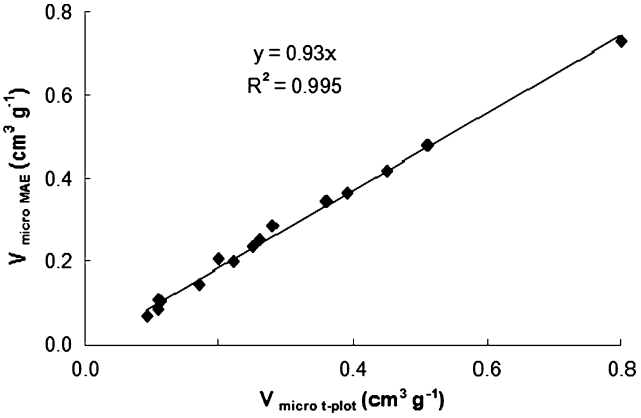

Fig. 10 Comparison between the microporous volumes determined by the MAE model and by the *t*-plot models for samples presented Table 4

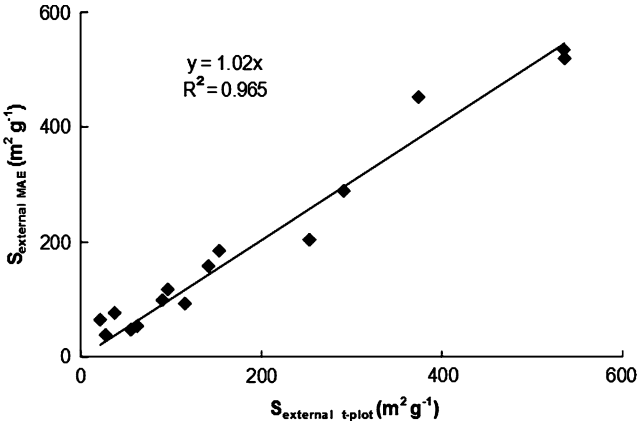

Fig. 11 Comparison between the external surfaces determined by the MAE model and by the *t*-plot models for samples presented Table 2

area of macroporous and some mesoporous solids. The fitting of isotherms for macroporous solids has led to promising results compared to those obtained with the BET model. Moreover, this model can also be used for an uncomplicated determination of porous volumes and external surfaces of microporous solids.

References

Amati, D., Kovats, E.S.: Nitrogen adsorption isotherms on organic and ionic model surfaces. Langmuir **3**, 687–695 (1987)

Anglin, E.J., Lingyun, C., Freeman, W.R., Sailor, M.J.: Porous silicon in drug delivery devices and materials. Adv. Drug Deliv. Rev. **60**, 1266–1277 (2008)

Anu Prathap, M.U., Srivastava, R.: Synthesis of nanoporous metal oxides through the self-assembly of phloroglucinol–formaldehyde resol and tri-block copolymer. J. Colloid Interface Sci. **358**, 399–408 (2011)

Astarita, G., Joshi, S.: Sample-dimension effects in the sorption of solvents in polymers—a mathematical model. J. Membr. Sci. **4**, 165–182 (1978)

Bartoszek, M., Eckelt, R., Jäger, C., Kosslick, H., Pawlik, A., Schulz, A.: Mesoporous silica-aluminas derived from precipitation: a study of the acidity, textural properties and catalytic performance. J. Mater. Sci. **44**, 6629–6636 (2009)

Blanco, J.F., Sublet, J., Nguyen, Q.T., Schaetzel, P.: Formation and morphology studies of different polysulfones-based membranes made by wet phase inversion process. J. Membr. Sci. **283**, 27–37 (2006)

Brunauer, S.: The Adsorption of Gases and Vapors. University Press, Oxford (1945)

Brunauer, S., Emmett, P.H.: Adsorption of gases in multimolecular layers. J. Am. Chem. Soc. **60**, 309–319 (1938)

de Boer, J.H., Lippens, B.C., Linsen, B.G., Broekhoff, J.C.P., van den Heuvel, A., Osinga, T.J.: The t-curve of multimolecular N_2 adsorption. J. Colloid Interface Sci. **21**, 405–414 (1966)

Dimitrov, L., Mihaylov, M., Hadjiivanov, K., Mavrodinova, V.: Catalytic properties and acidity of ZSM-12 zeolite with different textures. Microporous Mesoporous Mater. **143**, 291–301 (2011)

Emmett, P.H., Brunauer, S.: The use of low temperature van der Waals adsorption isotherms in determining the surface area of iron-synthetic ammonia catalysts. J. Am. Chem. Soc. **59**, 1553–1564 (1937)

Everett, D.H.: In: Unger, K.K., Rouquerol, J., Sing, K.S.W., Kral, H. (eds.) Characterisation of Porous Solids, pp. 1–22. Elsevier, Amsterdam (1998)

Favre, E., Clément, R., Nguyen, Q.T., Schaetzel, P., Néel, J.: Sorption of organic solvents into dense silicone membranes. J. Chem. Soc. Faraday Trans. **89**, 4339–4353 (1993)

Favre, E., Nguyen, Q.T., Clément, R., Schaetzel, P., Néel, J.: The engaged species induced clustering (ENSIC) model: a unified mechanistic approach of sorption phenomena in polymers. J. Membr. Sci. **117**, 227–236 (1996)

Flory, P.J.: Principles of Polymer Chemistry. Cornell University Press, Ithaca (1953)

Frackowiak, E.: Supercapacitors based on carbon materials and ionic liquids. J. Braz. Chem. Soc. **17**, 1074–1082 (2006)

Gregg, S.J., Sing, K.S.W.: Adsorption, Surface Area and Porosity, 2nd edn. Academic Press, London (1982)

Guzmán-Castillo, M.L., Armendáriz-Herrera, H., Pérez-Romo, P., Hernández-Beltrán, F., Ibarra, S., Valente, J.S., Fripiat, J.J.: Y zeolite depolymerization–recrystallization: simultaneous formation of hierarchical porosity and Na dislodging. Microporous Mesoporous Mater. **143**, 375–382 (2011)

Halsey, G.D.: Physical adsorption on non-uniform surfaces. J. Chem. Phys. **16**, 931–937 (1948)

Hill, T.L.: Theory of physical adsorption. Adv. Catal. **4**, 211–258 (1952)

Izquierdo-Barba, I., Sánchez-Salcedo, S., Colilla, M., José Feito, M., Ramírez-Santillán, C., Portolés, M.T., Vallet-Regí, M.: Inhibition of bacterial adhesion on biocompatible zwitterionic SBA-15 mesoporous materials. Acta Biomater. **7**, 2977–2985 (2011)

Jelinek, L., Kovhts, E.: True surface areas from nitrogen adsorption experiments. Langmuir **10**, 4225–4231 (1994)

Jura, G., Harkins, W.D.: Surfaces of solids. XI. Determination of the decrease (π) of free surface energy of a solid by an adsorbed film. J. Am. Chem. Soc. **66**, 1356–1373 (1944)

Keller, N., Pham-Huu, C., Ledoux, M.J., Estournes, C., Ehret, G.: Preparation and characterization of SiC microtubes. Appl. Catal. A, Gen. **187**, 255–268 (1999)

Lecloux, A., Pirard, J.P.: The importance of standard isotherms in the analysis of adsorption isotherms for determining the porous texture of solids. J. Colloid Interface Sci. **70**, 265–281 (1979)

Leite, E., Naydenova, I., Mintova, S., Leclercq, L., Toal, V.: Photopolymerisable nanocomposites for holographic recording and sensor application. Appl. Opt. **49**, 3652–3660 (2010)

Leofanti, G., Padovan, M., Tozzola, G., Venturelli, B.: Surface area and pore texture of catalysts. Catal. Today **41**, 207–219 (1998)

Lippens, B.C., DeBoer, J.H.: Studies on pore systems in catalysts: V. The *t* method. J. Catal. **4**, 319–323 (1965)

Marinovic, S., Vukovic, Z., Nastasovic, A., Milutinovic-Nikolic, A., Jovanovic, D.: Poly(glycidyl methacrylate-co-ethylene glycol dimethacrylate)/clay composites. Mater. Chem. Phys. **128**, 291–297 (2011)

McClellan, A.L., Hainsberger, H.F.: Cross-sectional areas of molecules adsorbed on solid surfaces. J. Colloid Interface Sci. **23**, 577–599 (1967)

Méndez, M.O.A., Lisbôa, A.C.L., Coutinho, A.R., Otani, C.: Activated petroleum coke for natural gas storage. J. Braz. Chem. Soc. **17**, 1144–1150 (2006)

Mikhail, R.S., Brunauer, S.: Surface area measurements by nitrogen and argon adsorption. J. Colloid Interface Sci. **52**, 572–577 (1975)

Moore, W.R., Shuttleworth, R.: Thermodynamic properties of solutions of cellulose acetate and cellulose nitrate. J. Polym. Sci., Part A, Gen. Pap. **1**, 733–749 (1963)

Passe-Coutrin, N., Altenor, S., Cossement, D., Jean-Marius, C., Gaspard, S.: Comparison of parameters calculated from the BET and Freundlich isotherms obtained by nitrogen adsorption on activated carbons: a new method for calculating the specific surface area. Microporous Mesoporous Mater. **111**, 517–522 (2008)

Payne, D.A., Sing, K.S.W., Turk, D.H.: Comparison of argon and nitrogen adsorption isotherms on porous and nonporous hydroxylated silica. J. Colloid Interface Sci. **43**, 287–293 (1973)

Pomonis, P.J., Petrakis, D.E., Ladavos, A.K., Kolonia, K.M., Pantazis, C.C., Giannakas, A.E., Leontiou, A.A.: The I-point method for estimating the surface area of solid catalysts and the variation of C-term of the BET equation. Catal. Commun. **6**, 93–96 (2005)

Ramila, A., Munoz, B., Perez-Pariente, J., Vallet-Reg, M.: Mesoporous MCM-41 as drug host system. J. Sol-Gel Sci. Technol. **26**, 1199–1202 (2003)

Ramsay, J.D.F.: In: Unger, K.K., Rouquerol, J., Sing, K.S.W., Kral, H. (eds.) Characterisation of Porous Solids, pp. 23–37. Elsevier, Amsterdam (1998)

Robinson, J.P., Tarleton, E.S., Millington, C.R., Nijmeijer, A.: Nanofiltration of organic solvents. Membr. Technol. **2004**, 5–12 (2004)

Rodrigues, A.E.: Permeable packings and perfusion chromatography in protein separation. J. Chromatogr. B **699**, 47–61 (1997)

Rodrigues, A.E., LeVan, M.D., Tondeur, D.: Adsorption, Science and Technology. Kluwer, Boston (1989)

Ruzicka, J., Kudlacek, L.: A study of the surface structure of cellulose by means of the argon adsorption isotherm. Vysokomol. Soyed. **6**, 577–586 (1964)

Scherdel, C., Reichenauer, G., Wiener, M.: Relationship between pore volumes and surface areas derived from the evaluation of N_2 sorption data by DR-, BET- and *t*-plot. Microporous Mesoporous Mater. **132**, 572–575 (2010)

Selles-Perez, M.J., Martin-Martinez, J.M.: Application of the αs method to adsorption isotherms of argon and n-butane. Carbon **30**(1), 41–46 (1992)

Sergio, M., Musso, M., Medina, J., Diano, W.: Aluminum-pillaring of a montmorillonitic clay: textural properties as a function of the starting mineral particle size. AZojomo (2006). doi:10.2240/azojomo0179

Serwicka, E.M.: Surface area and porosity, X-ray diffraction and chemical analyses. Catal. Today **56**, 335–346 (2000)

Sing, K.S.W., Williams, R.T.: Empirical procedures for the analysis of physisorption isotherms. Adsorp. Sci. Technol. **23**, 839–853 (2005)

Sing, K.S.W., Everett, D.H., Haul, R.A.W., Moscou, L., Pierotti, R.A., Rouquerol, J., Siemieniewska, T.: Reporting physisorption data for gas/solid systems with special reference to the determination of surface area and porosity. Pure Appl. Chem. **57**, 603–619 (1985)

Storck, S., Bretinger, H., Maier, W.F.: Characterization of micro- and mesoporous solids by physisorption methods and pore-size analysis. Appl. Catal. A, Gen. **174**, 137–146 (1998)

Thielmann, F., Butler, D.A., Williams, D.R.: Characterization of porous materials by finite concentration inverse gas chromatography. Colloids Surf. A, Physicochem. Eng. Asp. **187**, 267–272 (2001)

Trammell, S.A., Melde, B.J., Zabetakis, D., Deschamps, J.R., Dinderman, M.A., Johnson, B.J., Kusterbeck, A.W.: Electrochemical detection of TNT with in-line pre-concentration using imprinted diethylbenzene-bridged periodic mesoporous organosilicas. Sens. Actuators B, Chem. **155**, 737–744 (2011)

Whalley, W.R., Watts, C.W., Hilhorst, M.A., Bird, N.R.A., Balendonck, J., Longstaff, D.J.: The design of porous material sensors to measure the matric potential of water in soil. Eur. J. Soil Sci. **52**, 511–519 (2001)

Witoon, T., Chareonpanich, M., Limtrakul, J.: Effect of hierarchical meso-macroporous silica supports on Fischer-Tropsch synthesis using cobalt catalyst. Fuel Process. Technol. **92**, 1498–1505 (2011)

Yan, X., Liu, G., Dickey, M., Willson, C.G.: Preparation of porous polymer membranes using nano- or micro-pillar arrays as templates. Polymer **45**, 8469–8474 (2004)